

# Measurements of $\psi(2S)$ decays into $\phi\pi^0$ , $\phi\eta$ , $\phi\eta'$ , $\omega\eta$ , and $\omega\eta'$

M. Ablikim<sup>1</sup>, J. Z. Bai<sup>1</sup>, Y. Ban<sup>10</sup>, J. G. Bian<sup>1</sup>, X. Cai<sup>1</sup>, J. F. Chang<sup>1</sup>, H. F. Chen<sup>16</sup>, H. S. Chen<sup>1</sup>, H. X. Chen<sup>1</sup>, J. C. Chen<sup>1</sup>, Jin Chen<sup>1</sup>, Jun Chen<sup>6</sup>, M. L. Chen<sup>1</sup>, Y. B. Chen<sup>1</sup>, S. P. Chi<sup>2</sup>, Y. P. Chu<sup>1</sup>, X. Z. Cui<sup>1</sup>, H. L. Dai<sup>1</sup>, Y. S. Dai<sup>18</sup>, Z. Y. Deng<sup>1</sup>, L. Y. Dong<sup>1</sup>, S. X. Du<sup>1</sup>, Z. Z. Du<sup>1</sup>, J. Fang<sup>1</sup>, S. S. Fang<sup>2</sup>, C. D. Fu<sup>1</sup>, H. Y. Fu<sup>1</sup>, C. S. Gao<sup>1</sup>, Y. N. Gao<sup>14</sup>, M. Y. Gong<sup>1</sup>, W. X. Gong<sup>1</sup>, S. D. Gu<sup>1</sup>, Y. N. Guo<sup>1</sup>, Y. Q. Guo<sup>1</sup>, Z. J. Guo<sup>15</sup>, F. A. Harris<sup>15</sup>, K. L. He<sup>1</sup>, M. He<sup>11</sup>, X. He<sup>1</sup>, Y. K. Heng<sup>1</sup>, H. M. Hu<sup>1</sup>, T. Hu<sup>1</sup>, G. S. Huang<sup>1†</sup>, L. Huang<sup>6</sup>, X. P. Huang<sup>1</sup>, X. B. Ji<sup>1</sup>, Q. Y. Jia<sup>10</sup>, C. H. Jiang<sup>1</sup>, X. S. Jiang<sup>1</sup>, D. P. Jin<sup>1</sup>, S. Jin<sup>1</sup>, Y. Jin<sup>1</sup>, Y. F. Lai<sup>1</sup>, F. Li<sup>1</sup>, G. Li<sup>1</sup>, H. H. Li<sup>1</sup>, J. Li<sup>1</sup>, J. C. Li<sup>1</sup>, Q. J. Li<sup>1</sup>, R. B. Li<sup>1</sup>, R. Y. Li<sup>1</sup>, S. M. Li<sup>1</sup>, W. G. Li<sup>1</sup>, X. L. Li<sup>7</sup>, X. Q. Li<sup>9</sup>, X. S. Li<sup>14</sup>, Y. F. Liang<sup>13</sup>, H. B. Liao<sup>5</sup>, C. X. Liu<sup>1</sup>, F. Liu<sup>5</sup>, Fang Liu<sup>16</sup>, H. M. Liu<sup>1</sup>, J. B. Liu<sup>1</sup>, J. P. Liu<sup>17</sup>, R. G. Liu<sup>1</sup>, Z. A. Liu<sup>1</sup>, Z. X. Liu<sup>1</sup>, F. Lu<sup>1</sup>, G. R. Lu<sup>4</sup>, J. G. Lu<sup>1</sup>, C. L. Luo<sup>8</sup>, X. L. Luo<sup>1</sup>, F. C. Ma<sup>7</sup>, J. M. Ma<sup>1</sup>, L. L. Ma<sup>11</sup>, Q. M. Ma<sup>1</sup>, X. Y. Ma<sup>1</sup>, Z. P. Mao<sup>1</sup>, X. H. Mo<sup>1</sup>, J. Nie<sup>1</sup>, Z. D. Nie<sup>1</sup>, S. L. Olsen<sup>15</sup>, H. P. Peng<sup>16</sup>, N. D. Qi<sup>1</sup>, C. D. Qian<sup>12</sup>, H. Qin<sup>8</sup>, J. F. Qiu<sup>1</sup>, Z. Y. Ren<sup>1</sup>, G. Rong<sup>1</sup>, L. Y. Shan<sup>1</sup>, L. Shang<sup>1</sup>, D. L. Shen<sup>1</sup>, X. Y. Shen<sup>1</sup>, H. Y. Sheng<sup>1</sup>, F. Shi<sup>1</sup>, X. Shi<sup>10</sup>, H. S. Sun<sup>1</sup>, S. S. Sun<sup>16</sup>, Y. Z. Sun<sup>1</sup>, Z. J. Sun<sup>1</sup>, X. Tang<sup>1</sup>, N. Tao<sup>16</sup>, Y. R. Tian<sup>14</sup>, G. L. Tong<sup>1</sup>, G. S. Varner<sup>15</sup>, D. Y. Wang<sup>1</sup>, J. Z. Wang<sup>1</sup>, K. Wang<sup>16</sup>, L. Wang<sup>1</sup>, L. S. Wang<sup>1</sup>, M. Wang<sup>1</sup>, P. Wang<sup>1</sup>, P. L. Wang<sup>1</sup>, S. Z. Wang<sup>1</sup>, W. F. Wang<sup>1</sup>, Y. F. Wang<sup>1</sup>, Zhe Wang<sup>1</sup>, Z. Wang<sup>1</sup>, Zheng Wang<sup>1</sup>, Z. Y. Wang<sup>1</sup>, C. L. Wei<sup>1</sup>, D. H. Wei<sup>3</sup>, N. Wu<sup>1</sup>, Y. M. Wu<sup>1</sup>, X. M. Xia<sup>1</sup>, X. X. Xie<sup>1</sup>, B. Xin<sup>7</sup>, G. F. Xu<sup>1</sup>, H. Xu<sup>1</sup>, Y. Xu<sup>1</sup>, S. T. Xue<sup>1</sup>, M. L. Yan<sup>16</sup>, F. Yang<sup>9</sup>, H. X. Yang<sup>1</sup>, J. Yang<sup>16</sup>, S. D. Yang<sup>1</sup>, Y. X. Yang<sup>3</sup>, M. Ye<sup>1</sup>, M. H. Ye<sup>2</sup>, Y. X. Ye<sup>16</sup>, L. H. Yi<sup>6</sup>, Z. Y. Yi<sup>1</sup>, C. S. Yu<sup>1</sup>, G. W. Yu<sup>1</sup>, C. Z. Yuan<sup>1</sup>, J. M. Yuan<sup>1</sup>, Y. Yuan<sup>1</sup>, Q. Yue<sup>1</sup>, S. L. Zang<sup>1</sup>, Yu Zeng<sup>1</sup>, Y. Zeng<sup>6</sup>, B. X. Zhang<sup>1</sup>, B. Y. Zhang<sup>1</sup>, C. C. Zhang<sup>1</sup>, D. H. Zhang<sup>1</sup>, H. Y. Zhang<sup>1</sup>, J. Zhang<sup>1</sup>, J. Y. Zhang<sup>1</sup>, J. W. Zhang<sup>1</sup>, L. S. Zhang<sup>1</sup>, Q. J. Zhang<sup>1</sup>, S. Q. Zhang<sup>1</sup>, X. M. Zhang<sup>1</sup>, X. Y. Zhang<sup>11</sup>, Y. J. Zhang<sup>10</sup>, Y. Y. Zhang<sup>1</sup>, Yiyun Zhang<sup>13</sup>, Z. P. Zhang<sup>16</sup>, Z. Q. Zhang<sup>4</sup>, D. X. Zhao<sup>1</sup>, J. B. Zhao<sup>1</sup>, J. W. Zhao<sup>1</sup>, M. G. Zhao<sup>9</sup>, P. P. Zhao<sup>1</sup>, W. R. Zhao<sup>1</sup>, X. J. Zhao<sup>1</sup>, Y. B. Zhao<sup>1</sup>, Z. G. Zhao<sup>1\*</sup>, H. Q. Zheng<sup>10</sup>, J. P. Zheng<sup>1</sup>, L. S. Zheng<sup>1</sup>, Z. P. Zheng<sup>1</sup>, X. C. Zhong<sup>1</sup>, B. Q. Zhou<sup>1</sup>, G. M. Zhou<sup>1</sup>, L. Zhou<sup>1</sup>, N. F. Zhou<sup>1</sup>, K. J. Zhu<sup>1</sup>, Q. M. Zhu<sup>1</sup>, Y. C. Zhu<sup>1</sup>, Y. S. Zhu<sup>1</sup>, Yingchun Zhu<sup>1</sup>, Z. A. Zhu<sup>1</sup>, B. A. Zhuang<sup>1</sup>, B. S. Zou<sup>1</sup>.

(BES Collaboration)

<sup>1</sup> Institute of High Energy Physics, Beijing 100039, People's Republic of China

<sup>2</sup> China Center for Advanced Science and Technology (CCAST), Beijing 100080, People's Republic of China

<sup>3</sup> Normal University, Guilin 541004, People's Republic of China

<sup>4</sup> Henan Normal University, Xinxiang 453002, People's Republic of China

<sup>5</sup> Huazhong Normal University, Wuhan 430079, People's Republic of China

<sup>6</sup> Hunan University, Changsha 410082, People's Republic of China

<sup>7</sup> Liaoning University, Shenyang 110036, People's Republic of China

<sup>8</sup> Nanjing Normal University, Nanjing 210097, People's Republic of China

<sup>9</sup> Nankai University, Tianjin 300071, People's Republic of China

<sup>10</sup> Peking University, Beijing 100871, People's Republic of China

<sup>11</sup> Shandong University, Jinan 250100, People's Republic of China

<sup>12</sup> Shanghai Jiaotong University, Shanghai 200030, People's Republic of China

<sup>13</sup> Sichuan University, Chengdu 610064, People's Republic of China

<sup>14</sup> Tsinghua University, Beijing 100084, People's Republic of China

<sup>15</sup> University of Hawaii, Honolulu, Hawaii 96822, USA

<sup>16</sup> University of Science and Technology of China, Hefei 230026, People's Republic of China

<sup>17</sup> Wuhan University, Wuhan 430072, People's Republic of China

<sup>18</sup> Zhejiang University, Hangzhou 310028, People's Republic of China

\* Current address: University of Michigan, Ann Arbor, MI 48109, USA

† Current address: Purdue University, West Lafayette, Indiana 47907, USA.

Decays of the  $\psi(2S)$  into Vector plus Pseudoscalar meson final states have been studied with 14 million  $\psi(2S)$  events collected with the BESII detector. Branching fractions of  $\psi(2S) \rightarrow \phi\eta$ ,  $\phi\eta'$ , and  $\omega\eta'$ , and upper limits of  $\psi(2S) \rightarrow \phi\pi^0$  and  $\omega\eta$  are obtained:  $B(\psi(2S) \rightarrow \phi\eta) = (3.3 \pm 1.1 \pm 0.5) \times 10^{-5}$ ,  $B(\psi(2S) \rightarrow \phi\eta') = (3.1 \pm 1.4 \pm 0.7) \times 10^{-5}$ , and  $B(\psi(2S) \rightarrow \omega\eta') = (3.2^{+2.4}_{-2.0} \pm 0.7) \times 10^{-5}$ ; and  $B(\psi(2S) \rightarrow \phi\pi^0) < 0.40 \times 10^{-5}$ , and  $B(\psi(2S) \rightarrow \omega\eta) < 3.1 \times 10^{-5}$  at the 90 % C.L.. These results are used to test the pQCD “12% rule”.

PACS numbers: 13.25.Gv, 12.38.Qk, 14.40.Gx

## I. INTRODUCTION

It is expected in perturbative QCD that both  $J/\psi$  and  $\psi(2S)$  decays to light hadrons proceed dominantly via three gluons or a single virtual photon, with widths proportional to the squares of the  $c\bar{c}$  wave functions at the origin [1], which are well determined from dilepton decays [2]. This led to the “12% rule”, i.e.

$$Q_h = \frac{B(\psi(2S) \rightarrow h)}{B(J/\psi \rightarrow h)} \simeq \frac{B(\psi(2S) \rightarrow e^+e^-)}{B(J/\psi \rightarrow e^+e^-)} \simeq 12\%.$$

A strong violation of this conjecture was first observed by the MarkII experiment in the Vector-Pseudoscalar meson (VP) final states,  $\rho\pi$  and  $K^{*+}(892)K^-$  [3]. Significant suppressions observed in four Vector-Tensor decay modes ( $\omega f_2(1270)$ ,  $\rho a_2(1320)$ ,  $\phi f'_2$ , and  $K^*(892)\bar{K}^*(1430) + c.c.$ ) [4] make the puzzle even more mysterious. Numerous theoretical explanations have been suggested [5], but the puzzle still remains one of the most intriguing questions in charmonium physics. Recently both CLEO and BES reported new measurements of VP channels [6–8] with higher statistics and confirmed the severe suppression for  $\rho\pi$  and  $K^*(892)\bar{K} + c.c.$ .

In this letter, we report measurements of  $\psi(2S)$  decays into 5 VP channels:  $\phi\pi^0$ ,  $\phi\eta$ ,  $\phi\eta'$ ,  $\omega\eta$ , and  $\omega\eta'$  using 14 million  $\psi(2S)$  events collected with the BESII detector, where the branching fractions of  $\phi\eta'$  and  $\omega\eta'$  are the first observations. The results are compared with the corresponding  $J/\psi$  branching fractions to test the “12% rule”. Also, the branching fractions provide useful informations on DOZI suppressed decay  $\psi(2S) \rightarrow \phi\pi^0$  and on the quark components of  $\eta$  and  $\eta'$  [9].

## II. THE BESII DETECTOR

The Beijing Spectrometer (BESII) is a conventional cylindrical magnetic detector that is described in detail in Ref. [10]. A 12-layer Vertex Chamber (VC) surrounding the beryllium beam pipe provides input to the event trigger, as well as coordinate information. A forty-layer main drift chamber (MDC) located

just outside the VC yields precise measurements of charged particle trajectories with a solid angle coverage of 85% of  $4\pi$ ; it also provides ionization energy loss ( $dE/dx$ ) measurements which are used for particle identification. Momentum resolution of  $1.7\%\sqrt{1+p^2}$  ( $p$  in GeV/c) and  $dE/dx$  resolution for hadron tracks of  $\sim 8\%$  are obtained. An array of 48 scintillation counters surrounding the MDC measures the time of flight (TOF) of charged particles with a resolution of about 200 ps for hadrons. Outside the TOF counters, a 12 radiation length, lead-gas barrel shower counter (BSC), operating in limited streamer mode, measures the energies of electrons and photons over 80% of the total solid angle with an energy resolution of  $\sigma_E/E = 0.22/\sqrt{E}$  ( $E$  in GeV). A solenoidal magnet outside the BSC provides a 0.4 T magnetic field in the central tracking region of the detector. Three double-layer muon counters instrument the magnet flux return and serve to identify muons with momentum greater than 500 MeV/c. They cover 68% of the total solid angle.

In this analysis, a GEANT3 based Monte Carlo package with detailed consideration of the detector performance (such as dead electronic channels) is used. The consistency between data and Monte Carlo has been carefully checked in many high purity physics channels, and the agreement is reasonable [11].

## III. EVENT SELECTION

The data sample used for this analysis consists of  $(14.0 \pm 0.6) \times 10^6$   $\psi(2S)$  events [12], collected with BESII at the center-of-mass energy  $\sqrt{s} = m_{\psi(2S)}$ . The decay channels investigated are  $\psi(2S)$  into  $\phi\pi^0$ ,  $\phi\eta$ ,  $\phi\eta'$ ,  $\omega\eta$ , and  $\omega\eta'$ , where  $\phi$  decays to  $K^+K^-$ ,  $\omega$  to  $\pi^+\pi^-\pi^0$ ,  $\eta'$  to  $\eta\pi^+\pi^-$  or  $\gamma\pi^+\pi^-$ , and  $\pi^0$  and  $\eta$  to  $2\gamma$ . The events have either two or four charged tracks plus  $n$  ( $n \geq 1$ ) photons.

A neutral cluster is considered to be a photon candidate if the following requirements are satisfied: it is located within the BSC fiducial region, the energy deposited in the BSC is greater than 50 MeV, the first hit appears in the first 6 radiation lengths, the angle

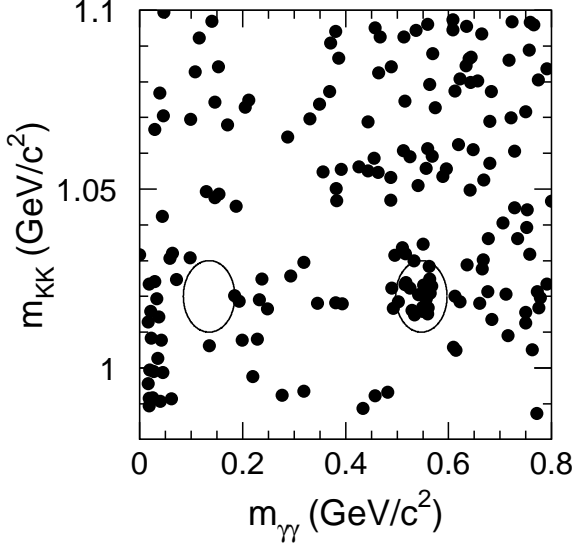


FIG. 1: Scatter plot of  $m_{KK}$  versus  $m_{\gamma\gamma}$  for  $\psi(2S) \rightarrow K^+K^-\gamma\gamma$  candidate events. The two ellipses in the plot indicate the  $2\sigma$  contours of the signal regions.

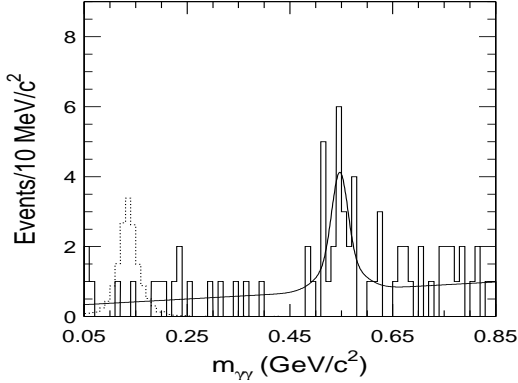


FIG. 2: Distribution of  $\gamma\gamma$  invariant mass for  $\psi(2S) \rightarrow \phi\gamma\gamma$  candidate events (solid histogram) and Monte Carlo simulation of  $\psi(2S) \rightarrow \phi\pi^0$  (dotted histogram) with arbitrary normalization. The curve shows the best fit described in the text.

in the  $xy$  plane (perpendicular to the beam direction) between the cluster and the nearest charged track is greater than  $16^\circ$  (this requirement is not applied for channels involving more than two photons), and the angle between the cluster development direction in the BSC and the photon emission direction from the beam interaction point (IP) is less than  $37^\circ$ .

Each charged track is required to be well fitted by a three-dimensional helix, to have a momentum transverse to the beam direction greater than  $70 \text{ MeV}/c$ , to originate from the IP region,  $V_{xy} = \sqrt{V_x^2 + V_y^2} < 2 \text{ cm}$  and  $|V_z| < 20 \text{ cm}$ , and to have a polar angle

$|\cos\theta| < 0.8$ . Here  $V_x$ ,  $V_y$ , and  $V_z$  are the  $x$ ,  $y$ , and  $z$  coordinates of the point of closest approach of the track to the beam axis.

The TOF and  $dE/dx$  measurements for each charged track are used to calculate  $\chi_{PID}^2(i)$  values and the corresponding confidence levels  $Prob_{PID}(i)$  for the hypotheses that a track is a pion, kaon, or proton, where  $i$  ( $i = \pi/K/p$ ) is the particle type. For events with  $\phi \rightarrow K^+K^-$  decays, charged kaon candidates are required to have  $Prob_{PID}(K)$  larger than 0.01 or larger than  $Prob_{PID}(\pi)$  and  $Prob_{PID}(p)$ ; while for events with  $\omega \rightarrow \pi^+\pi^-\pi^0$  decays, at least half of the charged pion candidates in each event are required to have  $Prob_{PID}(\pi) > 0.01$ .

#### A. $\psi(2S) \rightarrow \phi\pi^0$ and $\phi\eta$

The  $K^+K^-\gamma\gamma$  final state is utilized to measure these two channels. Two good charged tracks with net charge zero and at least two photon candidates are required. Next a four constraint (4C) kinematic fit ( $\chi_{kine}^2$ ) to the  $K^+K^-\gamma\gamma$  hypothesis is performed, and the confidence level of the fit is required to be larger than 0.01. If there are more than two photons, the fit is repeated using all permutations of photons, and the two photon combination with the minimum  $\chi_{kine}^2$  is selected. This procedure is used for all channels. To suppress backgrounds from  $\pi/K/p$  misidentification, the combined chisquare [13],  $\chi_{comb}^2$ , for the  $\psi(2S) \rightarrow K^+K^-\gamma\gamma$  assignment is required to be smaller than those of  $\psi(2S) \rightarrow \pi^+\pi^-\gamma\gamma$  and  $\psi(2S) \rightarrow p\bar{p}\gamma\gamma$ . Figure 1 shows the scatter plot of the invariant mass of  $K^+K^-$  ( $m_{K^+K^-}$ ) versus that of the two gammas ( $m_{\gamma\gamma}$ ). A clear cluster can be observed in the  $\phi\eta$  signal region, while only one event appears in the  $\phi\pi^0$  region.

To select  $\phi$  decay candidates, we require  $|m_{K^+K^-} - 1.02| < 0.02 \text{ GeV}/c^2$ . Here the experiment mass resolution for  $\phi$  is  $2.5 \text{ MeV}/c^2$ . The  $\gamma\gamma$  invariant mass distribution for events with  $\phi$  candidates is shown in Fig. 2. Fitting this distribution with  $\pi^0$  and  $\eta$  functions determined from Monte Carlo simulation, plus an  $\eta K^+K^-$  background determined by the sideband and a first order polynomial to describe phase space background,  $16.7 \pm 5.6 \phi\eta$  events are obtained with the statistical significance of  $3.6\sigma$  [14]. While for the  $\phi\pi^0$  channel, the observed events and the estimated background in the signal region are 4 and 6.2, respectively, which corresponds to the upper limit of  $4.4 \phi\pi^0$  events at the 90% confidence level [15].

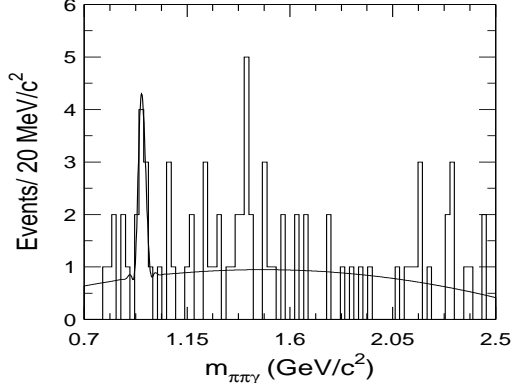


FIG. 3: The  $\gamma\pi^+\pi^-$  invariant mass distribution for  $\psi(2S) \rightarrow \phi\pi^+\pi^-\gamma$  candidate events. The curve shows the best fit described in the text.

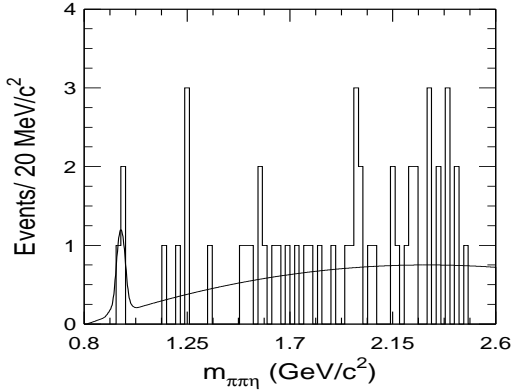


FIG. 4: The  $\pi^+\pi^-\eta$  invariant mass distribution for  $\psi(2S) \rightarrow \phi\pi^+\pi^-\eta$  candidate events. The curve shows the best fit described in the text.

### B. $\psi(2S) \rightarrow \phi\eta'$

Two decay modes of  $\eta'(958)$  are used,  $\eta'(958) \rightarrow \pi^+\pi^-\eta$  and  $\gamma\pi^+\pi^-$ . Their final states are  $K^+K^-\pi^+\pi^- + m\gamma$ , where  $m = 1$  for  $\eta' \rightarrow \gamma\pi^+\pi^-$  and  $m = 2$  for  $\eta' \rightarrow \pi^+\pi^-\eta$ ,  $\eta \rightarrow \gamma\gamma$ . Events with four charged tracks with net charge zero and at least  $m$  photon candidates are selected. A 4C kinematic fit is performed for the hypothesis  $\psi(2S) \rightarrow K^+K^-\pi^+\pi^-m\gamma$ , and the confidence level of the fit is required to be larger than 0.01. The corresponding  $\chi^2_{comb}$  for the  $\psi(2S) \rightarrow K^+K^-\pi^+\pi^-m\gamma$  assignment is required to be smaller than those of  $\psi(2S) \rightarrow \pi^+\pi^-\pi^+\pi^-m\gamma$  and  $\psi(2S) \rightarrow K^+K^-K^+K^-m\gamma$ .

The additional requirement  $|m_{K^+K^-} - 1.02| < 0.02$  GeV/c<sup>2</sup>, is used to select  $\phi$  candidates, and the  $m_{\gamma\pi^+\pi^-}$  spectrum of selected events is shown in Fig. 3. By fitting this spectrum with an  $\eta'$  function, plus an  $\eta'K^+K^-$  background determined by the sideband

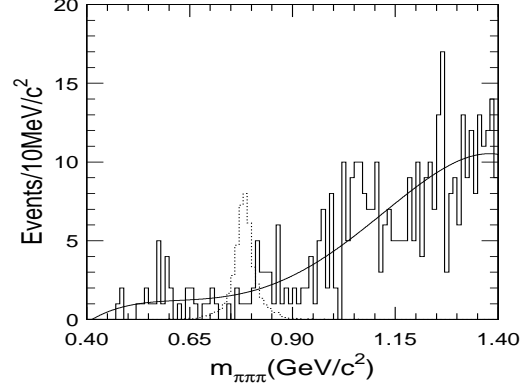


FIG. 5: The  $\pi^+\pi^-\pi^0$  invariant mass distribution for  $\pi^+\pi^-\pi^0\eta$  candidate events (solid histogram) and Monte Carlo simulation for  $\psi(2S) \rightarrow \omega\eta$  (dotted histogram) with arbitrary normalization. The curve shows the best fit described in the text.

and a second order polynomial for phase space background,  $5.8 \pm 3.2$   $\phi\eta'$  candidate events are obtained. The statistical significance is about  $2.0\sigma$ . Here, the shape of  $\eta'$  is determined from Monte Carlo simulation of  $\psi(2S) \rightarrow \phi\eta'$ ,  $\phi \rightarrow K^+K^-$ , and  $\eta' \rightarrow \gamma\pi^+\pi^-$ .

For the final state  $K^+K^-\pi^+\pi^-\gamma\gamma$ , the  $K^+K^-\pi^+\pi^-\eta$  candidate events are required to satisfy  $|m_{\gamma\gamma} - 0.547| < 0.05$  GeV/c<sup>2</sup>. Backgrounds from  $\psi(2S) \rightarrow \pi^+\pi^-J/\psi$ ,  $J/\psi \rightarrow \phi\eta$  and  $\psi(2S) \rightarrow \eta J/\psi$ ,  $J/\psi \rightarrow \phi\pi^+\pi^-$  are eliminated with two additional requirements  $|m_{recoil}^{\pi^+\pi^-} - 3.1| > 0.1$  GeV/c<sup>2</sup> and  $m_{K^+K^-\pi^+\pi^-} < 2.9$  GeV/c<sup>2</sup>, respectively.

With the requirement  $|m_{K^+K^-} - 1.02| < 0.02$  GeV/c<sup>2</sup>, the  $\pi^+\pi^-\gamma\gamma$  invariant mass distribution for  $\phi\pi^+\pi^-\eta$  candidate events is shown in Figure 4. Fitting the spectrum with an  $\eta'$  function plus a second order polynomial for background,  $2.6 \pm 1.8$   $\phi\eta'$  candidate events are obtained. The statistical significance is about  $2.0\sigma$ . The  $\eta'$  shape is determined from Monte Carlo simulation of  $\psi(2S) \rightarrow \phi\eta'$ ,  $\phi \rightarrow K^+K^-$  and  $\eta' \rightarrow \pi^+\pi^-\eta$ ,  $\eta \rightarrow \gamma\gamma$ .

### C. $\psi(2S) \rightarrow \omega\eta$

Here, the final state studied is  $\pi^+\pi^-\gamma\gamma\gamma\gamma$ . Events with two charged tracks with net charge zero and four or five photon candidates are selected. A 4C kinematic fit is performed for the hypothesis  $\psi(2S) \rightarrow \pi^+\pi^-\gamma\gamma\gamma\gamma$ , and the fit confidence level is required to be larger than 0.01. To remove background from  $\pi/K$  misidentification,  $\chi^2_{comb}$  is required to be smaller than that of  $\psi(2S) \rightarrow K^+K^-\gamma\gamma\gamma\gamma$ . Candidate events must satisfy  $|m_{\gamma_1\gamma_2} - 0.135| < 0.05$  GeV/c<sup>2</sup> and

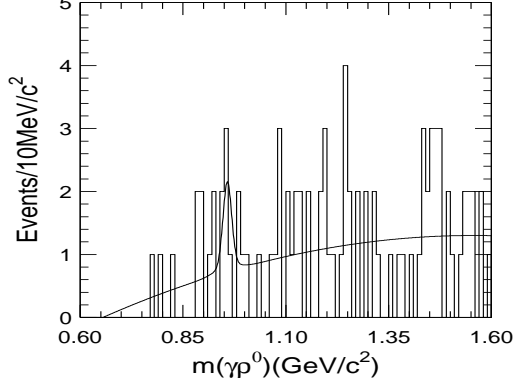


FIG. 6: The  $\gamma\pi^0$  invariant mass distribution for  $\psi(2S) \rightarrow \pi^+\pi^-\pi^+\pi^-\pi^0\gamma$  candidate events. The curve shows the best fit described in the text.

$|m_{\gamma\gamma_3\gamma_4} - 0.547| < 0.05 \text{ GeV}/c^2$  for the four photon candidates ( $\gamma_1\gamma_2\gamma_3\gamma_4$ ), where the subscripts permute over all six combinations. Events with one and only one combination satisfying the above criteria are kept for further analysis.

Figure 5 shows the  $\pi^+\pi^-\pi^0(m_{\pi\pi\pi})$  invariant mass distribution after the above selection; no clear  $\omega\eta$  signal is seen. The distribution is fitted with an  $\omega$  signal determined by Monte Carlo simulation and a polynomial background, the observed events and the estimated background in the signal region are 23 and 25.0, respectively, which corresponds to the upper limit of 9.7  $\omega\eta$  events at the 90% confidence level.

#### D. $\psi(2S) \rightarrow \omega\eta'$

Two  $\eta'(958)$  decay modes are used in this measurement, similar to the measurement of  $\psi(2S) \rightarrow \phi\eta'$ . Final states studied are  $\pi^+\pi^-\pi^+\pi^- + m\gamma$ , where  $m = 3$  for  $\eta' \rightarrow \gamma\pi^+\pi^-$  and  $m = 4$  for  $\eta' \rightarrow \eta\pi^+\pi^-$ . Events with four charged tracks with net charge zero and  $m$  or  $m + 1$  photons candidates are selected. A 4C kinematic fit to the hypothesis  $\psi(2S) \rightarrow \pi^+\pi^-\pi^+\pi^-m\gamma$  is performed, and its confidence level is required to be larger than 0.01 and larger than that of  $\psi(2S) \rightarrow K^+K^-\pi^+\pi^-m\gamma$  to suppress possible backgrounds due to particle misidentification. Backgrounds from  $\psi(2S) \rightarrow \pi^+\pi^-J/\psi$  are rejected with the requirement that the mass recoiling from every  $\pi^+\pi^-$  pair satisfy  $|m_{recoil}^{\pi^+\pi^-} - 3.1| > 0.05 \text{ GeV}/c^2$ .

For  $\pi^+\pi^-\pi^+\pi^-\gamma\gamma\gamma$ , one and only one pair among the three good photon candidates is required to satisfy  $|m_{\gamma\gamma} - 0.135| < 0.05 \text{ GeV}/c^2$ ; this pair is taken as a  $\pi^0$ . To avoid contamination from  $\psi(2S) \rightarrow \omega\pi^+\pi^-$ ,

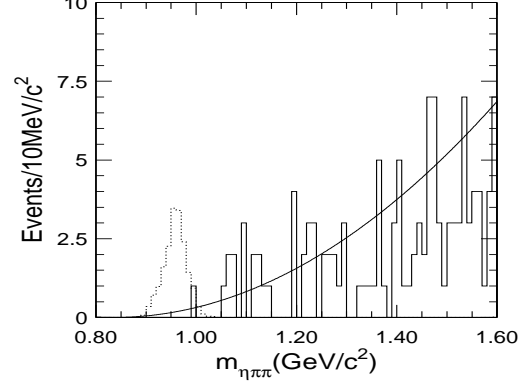


FIG. 7: The  $\eta\pi^+\pi^-$  invariant mass distribution for  $\psi(2S) \rightarrow \pi^+\pi^-\pi^+\pi^-\pi^0\eta$  candidate events (solid histogram) and Monte Carlo simulation of  $\psi(2S) \rightarrow \omega\eta', \eta' \rightarrow \pi^+\pi^-\eta$  (dotted histogram) with arbitrary normalization. The curve shows the best fit described in the text.

the  $\pi^+\pi^-\pi^0\pi^+\pi^-$  invariant mass should be less than 3.5 GeV. Since the dominant decay of  $\eta'$  into  $\gamma\pi^+\pi^-$  is  $\gamma\rho$ , an additional requirement  $|m_{\pi_1^+\pi_2^-} - 0.771| < 0.15 \text{ GeV}$  is applied to select  $\pi^+\pi^-\pi^0\gamma\rho$  candidates, where  $\pi_1^+\pi_2^-$  is any combination from the four charged pion candidates.

An additional requirement  $|m_{\pi^+\pi^-\pi^0} - 0.7826| < 0.05 \text{ GeV}/c^2$  is used to select  $\omega$  candidates. The  $\gamma\rho^0$  invariant mass spectrum for selected events is shown in Fig. 6. It is fitted with an  $\eta'$  function determined by Monte Carlo simulation for  $\psi(2S) \rightarrow \omega\eta', \eta' \rightarrow \gamma\rho$ , plus a second order polynomial for background, as shown in Fig. 6;  $4.2 \pm 2.7$  events are obtained with a statistical significance of  $1.9\sigma$ .

For the final state  $\pi^+\pi^-\pi^+\pi^-\gamma\gamma\gamma\gamma$ , the selection of  $\pi^0$  and  $\eta$  is the same as for the  $\omega\eta$  channel. Only events with only one  $\pi^0$  candidate ( $|m_{\gamma\gamma} - 0.135| < 0.05 \text{ GeV}/c^2$ ) and one  $\eta$  candidate ( $|m_{\gamma\gamma} - 0.547| < 0.05 \text{ GeV}/c^2$ ) from amongst the four photons are kept for further analysis.

An additional requirement  $|m_{\pi^+\pi^-\pi^0} - 0.7826| < 0.05 \text{ GeV}$  is made to select  $\omega$  candidates. The  $\eta\pi^+\pi^-$  invariant mass spectrum is shown in Fig. 7. It is fitted with an  $\eta'$  function determined by Monte Carlo simulation for  $\psi(2S) \rightarrow \omega\eta', \eta' \rightarrow \eta\pi^+\pi^-$ , plus a second order polynomial for background, as shown in Figure 7. With 1 event observed in the signal region and 3.2 background events estimated from sidebands, the candidate  $\omega\eta'$  signal is  $0_{-0}^{+1.7}$  event (at 68.3% C.L.) assuming the Poisson variate [15].

#### IV. SYSTEMATIC ERRORS

Many sources of systematic error are considered. Systematic errors associated with the efficiency are determined by comparing  $J/\psi$  and  $\psi(2S)$  data and Monte Carlo simulation for very clean decay channels, such as  $\psi(2S) \rightarrow \pi^+\pi^- J/\psi$ , which allows the determination of systematic errors associated with the MDC tracking, kinematic fitting, particle identification, and photon selection efficiencies [4, 11].

Since the decay  $\eta'$  to  $\gamma\pi^+\pi^-$  includes  $\gamma\rho^0$  and non-resonant  $\gamma\pi^+\pi^-$ , the  $\pi^+\pi^-$  invariant mass spectrum in the Monte Carlo simulation is obtained from  $J/\psi \rightarrow \gamma\eta'$ ,  $\eta' \rightarrow \gamma\pi^+\pi^-$  data. The uncertainty of their detection efficiency from  $\pi^+\pi^-$  invariant mass spectrum is 3%, which is included in systematic errors.

The uncertainties of the branching fractions of intermediate states, the background shapes in fitting, and the total number of  $\psi(2S)$  events are also sources of systematic errors. Table I summarizes the systematic errors for all channels.

Contributions from the continuum  $e^+e^- \rightarrow \gamma^* \rightarrow$  hadrons [16] are estimated using a data sample of  $6.42 \pm 0.24 \text{ pb}^{-1}$  taken at  $\sqrt{s} = 3.65 \text{ GeV}$  [17], corresponding to about one-third of the integrated luminosity at the  $\psi(2S)$ . Since no signal is observed for any channel analyzed, the continuum contribution and possible interference are not taken into consideration.

TABLE I: Summary of relative systematic errors (%).

	$\phi\pi^0$	$\phi\eta$	$\phi\eta'$	$\omega\eta$	$\omega\eta'$
Tracking	4.0	4.0	8.0	4.0	8.0
$\gamma$ selection	4.0	4.0	4.0	8.0	8.0
Kinematic fit	6.0	6.0	6.0	4.0	4.0
PID Efficiency	2.0	2.0	2.0	$\sim 0$	$\sim 0$
$\eta \rightarrow \gamma\rho$	—	—	1.9	—	1.9
Background shape	0.0	11.0	16.	0.0	18.9
MC statistics	1.4	2.1	1.8	1.3	2.0
Branching ratios	1.4	1.6	3.8	1.0	3.5
$N_{\psi(2S)}$	4.0				
Total	9.6	15.	21.	11.	23.

#### V. RESULTS AND DISCUSSION

The branching fraction for  $\psi(2S) \rightarrow X$  is calculated from

$$B(\psi(2S) \rightarrow X) = \frac{n_{\psi(2S) \rightarrow X \rightarrow Y}^{obs}}{N_{\psi(2S)} \cdot B(X \rightarrow Y) \cdot \epsilon^{MC}},$$

where X is the intermediate state, Y the final state, and  $\epsilon^{MC}$  the detection efficiency.

Table II summarizes the observed numbers of events, detection efficiencies, and branching fractions or upper limits for the channels studied. The branching fractions of  $\psi(2S) \rightarrow \phi\eta'$  and  $\psi(2S) \rightarrow \omega\eta'$  are calculated from the sum of events observed in the  $\eta' \rightarrow \gamma\rho$  and  $\eta\pi^+\pi^-$  channels, and an efficiency determined from the individual efficiencies weighted by the branching fractions of these two channels. The upper limit for  $\psi(2S) \rightarrow \omega\eta'$  branching fraction at 90% confidence level is  $9.2 \times 10^{-5}$ . For comparison, the table includes the corresponding branching fractions of  $J/\psi$  decays [2], as well as the ratios of the  $\psi(2S)$  to  $J/\psi$  branching fractions. Decays of  $\psi(2S)$  to  $\phi\eta$  and  $\omega\eta$  are suppressed by a factor of 2 and 12, respectively, compared with the 12% rule, while  $\phi\eta'$  and  $\omega\eta'$  are consistent with the rule within large errors. It is worth pointing out that the ratio of  $\frac{B(\phi\eta)}{B(\phi\eta')}$  is  $2.3 \pm 0.3$  and  $1.1 \pm 0.7$  for  $J/\psi$  and  $\psi(2S)$  decays, respectively, which are consistent within  $2\sigma$ , while the ratio of  $\frac{B(\omega\eta)}{B(\omega\eta')}$  is  $9.5 \pm 1.7$  for  $J/\psi$  decay, which is much larger than that of  $\psi(2S)$  decay.

This analysis without considering the continuum contribution (although not seen at present measurement) and possible interference might bring some uncertainty, which could only be clarified later by more accurate experiments such as CLEO-c or BESIII [18]. If the continuum contribution is treated incoherently, the continuum events, assuming the Poisson distribution, for  $\phi\eta$ ,  $\phi\eta'$  and  $\omega\eta'$  channels are  $0_{-0}^{+4.0}$  at 68.3% confidence level with the normalized integrated luminosity, this yields the branching fractions of  $\psi(2S) \rightarrow \phi\eta$ ,  $\phi\eta'$  and  $\omega\eta'$  to be  $(3.3_{-1.4}^{+1.1} \pm 0.5) \times 10^{-5}$ ,  $(3.1_{-2.0}^{+1.4} \pm 0.7) \times 10^{-5}$  and  $(3.2_{-3.2}^{+2.4} \pm 0.7) \times 10^{-5}$ , respectively.

In conclusion, the branching fractions for  $\psi(2S) \rightarrow \phi\eta$ ,  $\phi\eta'$ , and  $\omega\eta'$  and upper limits for  $\phi\pi^0$  and  $\omega\eta$  are presented. Our results for  $\phi\eta'$  and  $\omega\eta'$  are first measurements, while our results for  $\phi\pi^0$ ,  $\phi\eta$ , and  $\omega\eta$  are consistent with those of CLEO [6].

#### Acknowledgments

The BES collaboration thanks the staff of BEPC for their hard efforts. This work is supported in part by the National Natural Science Foundation of China under contracts Nos. 19991480, 10225524, 10225525, the Chinese Academy of Sciences under contract No. KJ 95T-03, the 100 Talents Program of CAS under Contract Nos. U-11, U-24, U-25, and the Knowledge Innovation Project of CAS under Contract Nos. U-602, U-34 (IHEP); by the National Natural Science Founda-

TABLE II: Branching fractions and upper limits (90% C.L.) measured for  $\psi(2S) \rightarrow \text{Vector} + \text{Pseudoscalar}$ . Results for corresponding  $J/\psi$  branching fractions [2] and the ratios  $Q_h = \frac{B(\psi(2S) \rightarrow h)}{B(J/\psi \rightarrow h)}$  are also given.

$h$	$N^{obs}$	$\epsilon$ (%)	$B(\psi(2S) \rightarrow)$ $\times 10^{-5}$	$B(J/\psi \rightarrow)$ $\times 10^{-4}$	$Q_h$ (%)
$\phi\pi^0$	$< 4.4$	16.1	$< 0.40$	$< 0.068$	—
$\phi\eta$	$16.7 \pm 5.6$	18.9	$3.3 \pm 1.1 \pm 0.5$	$6.5 \pm 0.7$	$5.1 \pm 1.9$
$\phi\eta'(\eta' \rightarrow \gamma\pi^+\pi^-)$	$5.8 \pm 3.2$	11.1			
$\phi\eta'(\eta' \rightarrow \eta\pi^+\pi^-)$	$2.6 \pm 1.8$	3.8			
$\phi\eta'(\text{combined})$	$8.4 \pm 3.7$	8.4	$3.1 \pm 1.4 \pm 0.7$	$3.3 \pm 0.4$	$9.4 \pm 4.8$
$\omega\eta$	$< 9.7$	6.3	$< 3.1$	$15.8 \pm 1.6$	$< 2.0$
$\omega\eta'(\eta' \rightarrow \gamma\pi^+\pi^-)$	$4.2 \pm 2.7$	2.6			
$\omega\eta'(\eta' \rightarrow \eta\pi^+\pi^-)$	$0.0^{+1.7}_{-0.0}$	1.8			
$\omega\eta'(\text{combined})$	$4.2^{+3.2}_{-2.7}$	2.3	$3.2^{+2.4}_{-2.0} \pm 0.7$	$1.67 \pm 0.25$	$19^{+15}_{-13}$

tion of China under Contract No. 10175060 (USTC);  
and by the Department of Energy under Contract No.

DE-FG03-94ER40833 (U Hawaii).

- 
- [1] T. Appelquist and H. D. Politzer, Phys. Rev. Lett. **34**, 43 (1975); A. De Rujula and S. L. Glashow, *ibid*, page 46.
- [2] Particle Data Group, S. Eidelman *et al.*, Phys. Lett. **B592**, 1 (2004), and references therein.
- [3] M. E. B. Franklin *et al.*, MarkII Collab., Phys. Rev. Lett. **51**, 963 (1983).
- [4] J. Z. Bai *et al.*, BES Collab., Phys. Rev. Lett. **81**, 5080 (1998).
- [5] W. S. Hou and A. Soni, Phys. Rev. Lett. **50**, 569 (1983); G. Karl and W. Roberts, Phys. Lett. **B144**, 243 (1984); S. J. Brodsky *et al.*, Phys. Rev. Lett. **59**, 621 (1987); M. Chaichian *et al.*, Nucl. Phys. **B323**, 75 (1989); S. S. Pinsky, Phys. Lett. **B236**, 479 (1990); X. Q. Li *et al.*, Phys. Rev. **D55**, 1421 (1997); S. J. Brodsky and M. Karliner, Phys. Rev. Lett. **78**, 4682 (1997); Yu-Qi Chen and Eric Braaten, Phys. Rev. Lett. **80**, 5060 (1998); M. Suzuki, Phys. Rev. **D63**, 054021 (2001); J. L. Rosner, Phys. Rev. **D64**, 094002 (2001); J. P. Ma, Phys. Rev. **D65**, 097506 (2002); M. Suzuki, Phys. Rev. **D65**, 097507 (2002).
- [6] N. E. Adam *et al.*, CLEO Collab., hep-ex/0407028.
- [7] M. Ablikim *et al.*, BES Collob., hep-ex/0407037.
- [8] M. Ablikim *et al.*, BES Collob., hep-ex/0408047.
- [9] L. Köpke and N. Wermes, Phys. Rep. **174**, 67 (1989)
- [10] J. Z. Bai *et al.*, BES Collab., Nucl. Instr. Meth. **A458**, 627 (2001).
- [11] J. Z. Bai *et al.*, BES Collab., Phys. Rev. **D70**, 012005 (2004).
- [12] X. H. Mo *et al.*, HEP&NP 28, 455(2004), hep-ex/0407055.
- [13] The combined  $\chi^2$ ,  $\chi^2_{comb}$ , is defined as the sum of the  $\chi^2$  values of the kinematic fit ( $\chi^2_{kine}$ ) and those from each of all particle identification assignments:  $\chi^2_{comb} = \sum_i \chi^2_{PID}(i) + \chi^2_{kine}$ .
- [14] The events number and statistical significance of the  $\phi\eta$  signal include the contribution from  $\psi(2S)$  decay and possibly from continuum, which is discussed in sections IV and V. This is also applicable for the  $\phi\eta'$  and  $\omega\eta'$  channels. The significance  $S$  is calculated by  $S = [-2 \times (\ln L_2 - \ln L_1)]^{1/2}$ , where  $L_1$  and  $L_2$  is the likelihood function value in the fit with and without signal, respectively.
- [15] J. Conrad *et al.*, Phys. Rev. **D67**, 012002 (2003). We use the modified likelihood ratio ordering including the systematic uncertainties of signal (Gaussian parametrization) and background (flat parametrization) in confidence interval construction.
- [16] P. Wang, C. Z. Yuan, X. H. Mo and D. H. Zhang, Phys. Lett. **B593**, 89 (2004); P. Wang, C. Z. Yuan and X. H. Mo, Phys. Rev. **D69**, 057502 (2004).
- [17] S. P. Chi, X. H. Mo and Y. S. Zhu, HEP& NP 28,1135(2004).
- [18] Preliminary Design Report of The BESIII Detector, IHEP-BEPCII-SB-13, January, 2004.